Gauche, Ortho, and Anti Conformations of Saturated A_4X_{10} Chains: When Will All Six Conformers Exist?

Frank Neumann,[†] Hiroyuki Teramae,[‡] John W. Downing,[†] and Josef Michl*,[†]

Contribution from the Department of Chemistry and Biochemistry, University of Colorado, Boulder, Colorado 80309-0215, and NTT Basic Research Laboratories, Morinosato, Atsugi, Kanagawa 243-01, Japan

Received May 2, 1997

Abstract: Geometries of A_4X_{10} molecules (A = C, Si; X = H, F, Cl, Br, CH_3, SiH_3) have been optimized at the HF/6-31G* level as a function of the AAAA dihedral angle ω. In addition to the generally known gauche and trans conformational minima, some have an additional ("ortho") minimum near $\omega = 90°$. This appears only within a certain critical range of sizes of substituents X. It is attributed to a splitting of the ordinary gauche minimum by 1,4 interactions between substituents, similarly as the twisting of the anti minimum from 180° is attributable to 1,3 interactions. A universal model is proposed to rationalize the appearance and subsequent disappearance of the ortho minimum as X increases in size. It contains intrinsic barriers described according to Weinhold, van der Waals interactions described by a Lennard-Jones 6−12 potential, and Coulomb charge−charge interactions.

Introduction

Conformational properties of flexible linear chains are of fundamental importance in determining the behavior of organic molecules and are among the first pieces of information presented in elementary textbooks of organic chemistry and polymer science. They are also important for compounds of elements other than carbon, such as silicon.

It is commonly assumed that saturated linear chains A_nX_{2n+2} are capable of existing in only three distinct stable conformer forms with respect to rotation around a skeletal A−A bond: two enantiomeric gauche forms (g_+, g_-) with AAAA dihedral angles ω of about 60° (right-handed helix) and −60° (left-handed helix), and an anti form (a) with ω of 180° [1] (as in polyethylene[2]). In the anti form, deviations of ω up or down from 180° occur for substituents X larger than H, and have been attributed to steric interference between substituents in positions 1 and 3 in the ideally staggered backbone ("1,3 interactions"). The anti minimum is then split into a pair of enantiomeric minima (a_+, a_-), forcing a helical arrangement of the A atoms in the all-anti form[3] (as in poly(tetrafluoroethylene)[2]).

The existence of a total of four conformers with respect to rotation around a central A−A bond (g_+, g_-, a_+, a_-) is thus generally considered the norm, although it is recognized that extremely sterically encumbered structures may display exceptional behavior.[4] However, at irregular intervals throughout the past few decades, computational evidence for yet another pair of conformers, with a minimum near $\omega = \pm 90°$, has been reported for some relatively unhindered saturated linear chains, making for a total of six conformers. Until recently, these calculations were so approximate that limited significance and/or generality appears to have been attached to them by their authors or anyone else [CNDO/2 for $(CF_2)_n$,[5] MM2 for C_4Me_{10}[6], MM2[7] and MNDO/2[8] for Si_nH_{2n+2} and Si_nMe_{2n+2}]. Numerous other calculations of linear chain conformations only found the usual three or four conformers.[9a,10] At times, the existence of only three or four conformers was assumed and geometry optimization was restricted to limited dihedral angles.[11] In a few cases it was noted that the dihedral angle ω computed for the "gauche" minimum was curiously far from ±60° and closer to ±90°.[12] Until recently, the only experimental evidence for the existence of a conformational minimum at ±90° that we are aware of were several unexpected dihedral angles close

[†] University of Colorado.

[‡] Morinosato.

(1) Eliel, E. L.; Wilen, S. H. *Stereochemistry of Organic Compounds*; Wiley: Chichester, UK, 1994.

(2) Bovey, F. A.; Kwei, T. K. In *Macromolecules, An Introduction to Polymer Science*; Bovey, F. A., Winslow, F. H., Eds.; Academic Press: New York, 1979; p 260.

(3) Boyd, R. H.; Philips, P. J. *The Science of Polymer Molecules*; Cambridge University Press: Cambridge, 1993.

(4) E.g.: Beckhaus, H.-D.; Hellmann, G.; Rüchardt, C. *Chem. Ber.* **1978**, *111*, 72. Hounshell, W. D.; Dougherty, D. A.; Mislow, K. *J. Am. Chem. Soc.* **1978**, *100*, 3149.

(5) Morokuma, K. *J. Chem. Phys.* **1971**, *54*, 962.

(6) Beckhaus, H. D.; Rüchardt, C.; Anderson, J. E. *Tetrahedron* **1982**, *38*, 2299. The related splitting of the g_+g_- minimum in *n*-pentane was recognized in: Dale, J. *Stereochemistry and Conformational Analysis*; Universitetsforlaget: Oslo, Norway, 1978; p 98.

(7) Welsh, W. J.; Debolt, L.; Mark, J. E. *Macromolecules* **1986**, *19*, 2987.

(8) Welsh, W. J.; Johnson, W. D. *Macromolecules* **1990**, *23*, 1881.

(9) Hehre, W. J.; Radom, L.; Schleyer, P. v. R.; Pople, J. A. *Ab Initio Molecular Orbital Theory*; Wiley: New York, 1985; (a) p 261, (b) p 80.

(10) Berg, U.; Sandstrom, J. *Adv. Phys. Org. Chem.* **1989**, 25, 1. Rosenthal, L.; Rabolt, J. F.; Hummel, J. *J. Chem. Phys.* **1982**, *76*, 817. Wiberg, K. B.; Murcko, M. A. *J. Am. Chem. Soc.* **1988**, *110*, 8029. Osawa, E.; Shirahama, H.; Matsumoto, T. *J. Am. Chem. Soc.* **1979**, *101*, 4824. Osawa, E.; Collins, J. B.; Schleyer, P. v. R. *Tetrahedron* **1977**, *33*, 2667. Anderson, J. E.; Pearson, H. *Tetrahedon Lett.* **1972**, 2779. Damewood, J. R., Jr.; West, R. *Macromolecules* **1985**, *18*, 159. Farmer, B. L.; Rabolt, J. F.; Miller, R. D. *Macromolecules* **1987**, *20*, 1167. Ortiz, J. V.; Mintmire, J. W. *J. Am. Chem. Soc.* **1988**, *110*, 4522. Mintmire, J. W. *Phys. Rev. B* **1989**, *39*, 13350. Teramae, H.; Takeda, K. *J. Am. Chem. Soc.* **1989**, *111*, 1281. Cui, C. X.; Karpfen, A.; Kertesz, M. *Macromolecules* **1990**, *23*, 3302. Jalali-Heravi, M.; McManus, S. P.; Zutaut, S. E.; McDonald, J. K. *Chem. Mater.* **1991**, *3*, 1024. Welsh, W. J. *Adv. Polym. Technol.* **1993**, *12*, 379.

(11) Janoschek, R.; Stueger, H. *J. Mol. Struct. (THEOCHEM)* **1994**, *119*, 83.

(12) Otto, P.; Ladik, J.; Förner, W. *Chem. Phys.* **1985**, *95*, 365. Plitt, H. S.; Michl, J. *Chem. Phys. Lett.* **1992**, *198*, 400. Plitt, H. S.; Downing, J. W.; Raymond, M. K.; Balaji, V.; Michl, J. *J. Chem. Soc., Faraday Trans.* **1994**, *90*, 1653.

S0002-7863(97)01406-6 CCC: $15.00 © 1998 American Chemical Society
Published on Web 01/13/1998

to 90° in the X-ray structure of a macrocyclic compound, $Si_{16}Me_{32}$;[13] additional examples have since been found in branched oligosilanes.[14]

Our interest in the subject stems from efforts to understand the conformational dependence of the optical properties of oligosilanes and polysilanes.[15] We were initially confirmed in the usual skeptical attitude toward the possible existence of a third pair of conformers when our MP2/6-31G** calculations[16] for Si_4H_{10} provided no evidence for it, although earlier semiempirical calculations[8] affirmed its presence clearly. It seemed to us that the isolated reports of a third pair were artifacts of crude computational methods. Although this is so in the case of Si_4H_{10}, we now know that, in general, we were wrong.

A 3-21G* calculation for Si_4Me_{10} at the fully optimized Hartree−Fock and single-point MP2 levels,[17] followed by fully optimized 6-31G* calculations at both HF and MP2 levels,[18] and also a D95+* calculation for C_4F_{10} at the fully optimized Hartree−Fock level,[19] followed by a fully optimized MP2/6-31G* calculation,[20,21] all agreed with those previous more approximate calculations for $(SiMe_2)_n$[7,8] and $(CF_2)_n$[5] chains that predicted the existence of a third backbone conformer pair ($\omega \simeq 90°$) in addition to the usual gauche and anti pairs. The energies of the three conformer pairs were always within 2 or 3 kcal/mol of each other. The MP2/6-31G* results paralleled the HF/6-31G* results very closely. We then obtained the same result for $C_4(CH_3)_{10}$ at the fully optimized HF/6-31G* level (mentioned in a footnote in ref 20), in agreement with a prior MM2 report.[6]

These ab initio results were not easily dismissed, since the levels of calculation employed are generally fairly reliable for molecular conformations, and also since Smith et al.[19] showed that the use of a six-minima torsional potential in the rotational isomeric state model of polymer properties accounted for the behavior of poly(tetrafluoroethylene) better than the use of the standard four-minima potential. An observation[20,21] of three distinct IR spectra of the individual conformers of C_4F_{10} in nitrogen matrix removed any remaining doubt: at least in some A_4X_{10} chains, there indeed are three pairs of backbone conformations at comparable energies. The next questions are, why and when?

Smith et al. suggested[19] that the splitting of the expected "ordinary gauche" pair of minima at ±60° into a pair at about ±55° and another at about ±90° in C_4F_{10} is due to steric 1,4 interactions (i.e., interactions between substituents located in backbone positions 1 and 4), and is entirely analogous to the splitting of the *a* minimum into a_+ and a_- minima, believed to be due to the above-mentioned 1,3 interactions. Although they did not consider other chains, this sounds like a general argument, and it appeared to us that a total of six conformational minima in the ground-state potential energy surface ought to be the rule for most if not all molecules of the type A_4X_{10}, except for the smallest substituents X and the longest bond lengths A−A. At this point, we were truly curious and decided to perform fully optimized conformational search calculations for a series of saturated linear chains A_4X_{10}.

We were initially rather perplexed by the results, since the calculations sometimes produced only the usual two pairs of conformations even for quite large substituents X. As qualitative understanding of open chain conformations would appear to be a rather fundamental requirement in elementary stereochemistry, it appeared desirable to find a very simple model that would rationalize or perhaps even predict the number of conformations for an A_4X_{10} chain from elementary properties of the atom A and the group X without having to resort to an extensive computer calculation. Presently, we report the results of this search for the origin of the conformational diversity.

For simplicity, we use the "ortho" (o_+, o_-) designation for the third conformer pair, proposed in the experimental study of C_4F_{10} in recognition of the computed near orthogonality of the dihedral angle ω,[20] and not the g_+^+, g_+^- labels proposed by Smith et al.[19]

Methods of Calculation

All computations were performed with IBM RS 6000/550 and 590 work stations.

***Ab Initio* Calculations of Conformer Geometries and Energies.** These used the GAUSSIAN 92 program.[22] Calculations for C_4X_{10} and Si_4X_{10} [X = H, F, Cl, Br (only C_4Br_{10}), CH_3(=Me), and SiH_3] were done at the HF/6-31G* level.[23] HF calculations for C_4Br_{10} used an effective core potential (ECP).[24] Calculations for Si_4F_{10} were also repeated at the MP2/6-31G* level, and those for C_4Cl_{10} at the HF/6-311G* level. The results for Si_4H_{10} and Si_4Me_{10} were taken from refs 16 and 18, respectively. Atomic charges were obtained from natural bond orbital (NBO)[25] and Mulliken population analyses.

Geometry optimizations for a series of fixed central dihedral angles under the assumption of C_2 symmetry yielded potential energy curves. They were followed by unconstrained optimizations for the minima found in these curves. Frequency analysis was performed at all fully optimized geometries, except for C_4Br_{10}, $Si_4(SiH_3)_{10}$, and the MP2 calculation on Si_4F_{10}, where our computational resources were insufficient.

A C_2 symmetry axis was found in each case and the potential energy curves (Figure 1) thus correspond to minimum energy paths in the vicinity of potential energy minima. This need not be the case in the regions of high energy. As first shown by Dewar and Kirschner,[26] "chemical hysteresis" may cause a path obtained by gradually changing the value of one geometrical parameter, while optimizing all the others, to stray far from the lowest energy path. The computed transition energies will then be too high. This behavior is suspected in Si_4Me_{10},[18]

(13) Shafiee, F.; Haller, K. J.; West, R. *J. Am. Chem. Soc.* **1986**, *108*, 5478.

(14) Lambert, J. B.; Pflug, J. L.; Stern, C. L. *Angew. Chem., Int. Ed. Engl.* **1995**, *34*, 98. Lambert, J. B.; Pflug, J. L.; Allgeier, A. M.; Campbell, D. J.; Higgins, T. B.; Singewald, E. T.; Stern, C. L. *Acta Crystallogr. C* **1995**, *C51*, 713. Lambert, J. B.; Pflug, J. L.; Denari, J. M. *Organometallics* **1996**, *15*, 615. Pflug, J. L. Ph.D. Dissertation, Northwestern University, Evanston, IL, 1994. Sekiguchi, A.; Nanjo, M.; Kabuto, C.; Sakurai, H. *J. Am. Chem. Soc.* **1995**, *117*, 4195.

(15) Miller, R. D.; Michl, J. *Chem. Rev.* **1989**, *89*, 1359. Imhof, R.; Antic, D.; David, D. E.; Michl, J. *J. Phys. Chem. A* **1997**, *101*, 4579. Imhof, R.; Teramae, H.; Michl, J. *Chem. Phys. Lett.* **1997**, *270*, 500. Mazières, S.; Raymond, M. K.; Raabe, G.; Prodi, A.; Michl, J. *J. Am. Chem. Soc.* **1997**, *119*, 6682.

(16) Albinsson, B.; Teramae, H.; Plitt, H. S.; Goss, L. M.; Schmidbaur, H.; Michl, J. *J. Phys. Chem.* **1996**, *100*, 8681.

(17) Teramae, H.; Michl, J. *Mol. Cryst. Liq. Cryst.* **1994**, *256*, 149.

(18) Albinsson, B.; Teramae, H.; Downing, J. W.; Michl, J. *Chem. Eur. J.* **1996**, *2*, 529.

(19) Smith, G. D.; Jaffe, R. L.; Yoon, D. Y. *Macromolecules* **1994**, *27*, 3166.

(20) Albinsson, B.; Michl, J. *J. Am. Chem. Soc.* **1995**, *117*, 6378.

(21) Albinsson, B.; Michl, J. *J. Phys. Chem.* **1996**, *100*, 3418.

(22) GAUSSIAN 92, Revision C, Frisch, M. J.; Trucks, G. W.; Head-Gordon, M.; Gill, P. M. W.; Wong, M. W.; Foresman, J. B.; Johnson, B. G.; Schlegel, H. B.; Robb, M. A.; Replogle, E. S.; Gomperts, R.; Andres, J. L.; Raghavachari, K.; Binkley, J. S.; Gonzales, C.; Martin, R. S.; Fox, D. J.; Defrees, D. J.; Baker, J.; Stewart, J. J. P.; Pople, J. A. Gaussian Inc.: Pittsburgh, PA, 1992.

(23) Hariharan, P. C.; Pople, J. A. *Theor. Chim. Acta* **1973**, *28*, 213. Ditchfield, R.; Hehre, W. J.; Pople, J. A. *J. Chem. Phys.* **1971**, *54*, 724. Hehre, W. J.; Ditchfield, R.; Pople, J. A. *J. Chem. Phys.* **1972**, *56*, 2257. Gordon, M. S. *Chem. Phys. Lett.* **1980**, *76*, 163.

(24) Bergner, A.; Dolg, M.; Küchle, W.; Stoll, H.; Preuss, H. *Mol. Phys.* **1993**, *80*, 1431. Kaupp, M.; Schleyer, P. v. R.; Stoll, H.; Preuss, H. *J. Am. Chem. Soc.* **1991**, *113*, 6012.

(25) NBO 4.0; Glendening, E. D.; Badenhoop, J. K.; Reed, A. J.; Carpenter, J. E.; Weinhold, F.; Theoretical Chemical Institute, University of Wisconsin: Madison, WI, 1994.

(26) Dewar, M. J. S.; Kirschner, S. *J. Am. Chem. Soc.* **1971**, *93*, 4292.

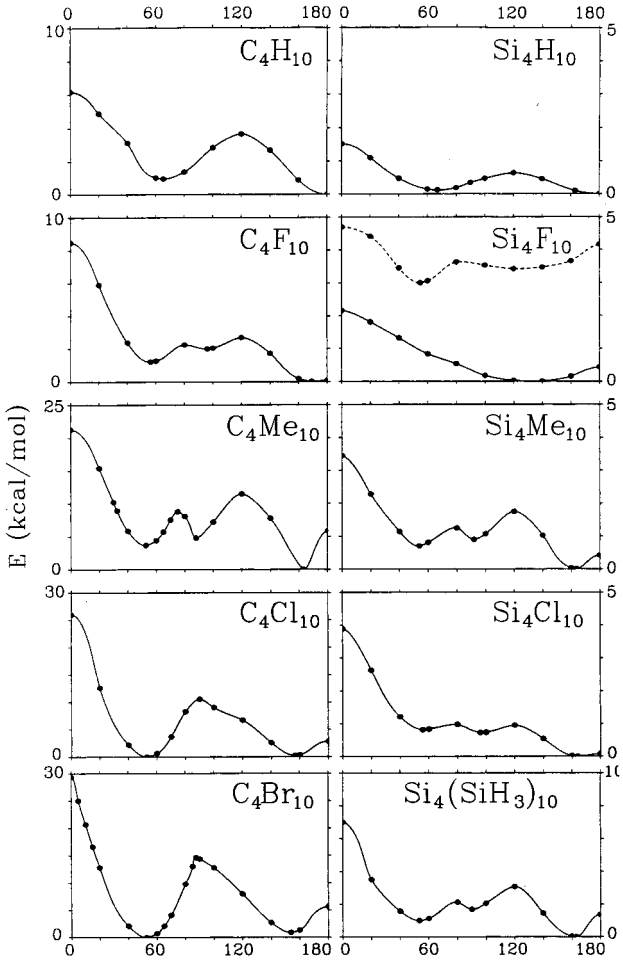

Figure 1. Optimized HF/6-31G* potential energy of A_4X_{10} chains as a function of the dihedral angle ω. C_2 symmetry was assumed except as stated in the text for C_4Me_{10}. The dashed MP2/6-31G* curve in Si_4F_{10} is shifted arbitrarily relative to the HF/6-31G* curve.

and we now find it in the one case that was examined in some detail, C_4Me_{10}. Here, the barrier between the ortho and gauche minima appears to occur at $\omega = 60°$ if approached along the bottom of a valley from larger ω values and at 80° if approached along the bottom of a parallel valley from smaller ω values. The two valleys differ in the sense of rotation of the terminal backbone bonds. The true transition structure was not located. It seems to lie on the ridge separating the two valleys, at a dihedral angle ω of about 75°, and does not possess C_2 symmetry, i.e., the end groups rotate independently. To obtain this region of the curve shown in Figure 1, we drove one of the terminal rotation angles while holding ω constant at 75° and optimizing all other geometrical variables without symmetry constraints. The true activation energy is thus lower than shown in Figure 1. The relaxation of the C_2 symmetry constraint may lower the barriers between conformers in the other A_4X_{10} molecules as well, and the exploration of transition states in linear chain conformational isomerization deserves a separate study.

Although substituent conformations are of limited relevance for our primary goal, which is an understanding of backbone conformations, we note that there might in principle be many different local minima on a A_4Me_{10} hypersurface with nearly identical AAAA dihedral angles and differently rotated methyl groups. In the highly crowded C_4Me_{10}, where we observe coupled rotation of the methyl groups in the sense of the previously reported[6,33] gearing motions, and maybe in $Si_4(SiH_3)_{10}$ as well, the appearance of multiple local minima due to methyl rotation is less likely than in the less crowded Si_4Me_{10}. We have not observed such multiple minima in our ab initio calculations for any of these molecules, nor in numerous molecular mechanics calculations performed in preliminary searches.

Model Calculations. The potential energy was the sum of (i) the intrinsic barrier, present even in ethane, (ii) the van der Waals interaction among the 10 substituents, and (iii) the electrostatic interactions among the 14 A and X atoms and substituents.

Table 1. Substituent van der Waals Radii

substituent	r^{vdW} (Å)[a]	substituent	r^{vdW} (Å)[a]
H	1.20	Cl	1.75
F	1.47	Br	1.85
Me	~1.70[b]	SiH_3	~2.20[b]

[a] Reference 29. [b] Calculated from the geometries of CH_3 and SiH_3.

(i) An empirical function was used for the intrinsic part of the barrier. This function was derived by the Weinhold procedure[27] based on the effects of the deletion of elements in the Fock matrix expressed in the natural bond orbital basis, as implemented in the NBO part of the GAUSSIAN 92 program.[25] For rotation around the central A−A bond (angle ω, positive for counterclockwise rotation at the closer atom A, i.e., right-handed AAAA helix), the elements deleted were those between the two A−X and the A(2)−A(1) bond orbitals on atom 2 and the two A−X and the A(3)−A(4) antibond orbitals on atom 3, plus the analogous ones between the bond orbitals on atom 3 and antibond orbitals on atom 2. For rotation around the terminal bonds (angle ϕ, zero at the staggered geometry and positive for counterclockwise rotation of the terminal groups when viewed from a point located on the terminal bond axis outside the molecule), the elements deleted were those between the three A−X bonds on the terminal atoms A(1) and A(4) with the central A(2)−A(3) antibond and the A−X antibonds on central atoms A(2) and A(3), respectively, and the analogous ones between the antibond orbitals on A(1) and A(4) with the bond orbitals on A(2) and A(3). The intrinsic function was fitted to the forms $(C/2)(1 + \cos(3\omega))$ and $C(1 - \cos(3\phi))$ for rotation around the central bond and simultaneous rotations around both terminal bonds, respectively. A universal value $C = 4.5$ kcal/mol simulated all the ab initio results semiquantitatively. Only Si_4F_{10} stands apart as the shape of the intrinsic barrier of its central bond is totally different, and no attempt was made to fit it to a functional form.

(ii) The Lennard-Jones 6−12 potential[28] was used for van der Waals interactions. The van der Waals radii[29] r_X^{vdW} used are collected in Table 1. We are aware of the ambiguities[30] involved in the definition of r_X^{vdW} but believe that they will not invalidate the model as long as a consistent set of values is used. A universal proportionality constant $\epsilon = 0.012$ kcal/mol was found to provide a semiquantitative fit with all the ab initio results.

(iii) Point charge repulsions were used for electrostatic interactions. Charge $Q_X = q_X$ was placed on each substituent X, $Q_A = -2q_X$ on central atoms A, and $Q_A = -3q_X$ on terminal atoms A, with q_X equal to the average value on the 10 substituents from ab initio calculations by either the Weinhold NBO or Mulliken procedure. Charges on a polyatomic substituent were collapsed into a point charge at the atom attached to the chain.

The final expression for energy (in kcal/mol) as a function of ω and ϕ was

$$E_{TOT} = E_{INTR} + E_{vdW} + E_{COUL}$$

$$E_{INTR} = (C/2)(3 + \cos(3\omega) - 2\cos(3\phi))$$

$$E_{vdW} = \epsilon \sum_{i<j\{X\}} [(2r_X^{vdW}/r_{i-j})^{12} - (2r_X^{vdW}/r_{i-j})^6]$$

(27) Reed, A. E.; Weinhold, F. *Israel J. Chem.* **1991**, *31*, 277.
(28) Berry, R. S.; Rice, S. A.; Ross, J. *Physical Chemistry*; Wiley: New York, 1981; pp 418 and 785. Lennard-Jones, J. E. *Proc. Phys. Soc.* **1931**, *43*, 461.
(29) Bondi, A. *J. Phys. Chem.* **1964**, *68*, 441.
(30) Allinger, N. L.; Miller, M. A.; VanCatledge, F. A.; Hirsch, J. A. *J. Am. Chem. Soc.* **1967**, *89*, 4345.

$$E_{COUL} = (1/4\pi\epsilon_0) \sum_{i<j\{A,X\}} Q_i Q_j / r_{i-j}$$

where i and j run over the substituents X or both over the chain atoms A and substituents X, as indicated by {X} and {A,X}, respectively, and r_{i-j} is the distance between atoms i and j. With angles in degrees, distances in Å, charges in elementary units, and energy in kcal/mol, the values of the constants are $C = 4.5$, $\epsilon = 0.012$, and $1/4\pi\epsilon_0 = 332.064$.

In each A_4X_{10} chain, all backbone bond lengths r_{A-A} were assumed equal, as were all backbone-to-substituent bond lengths r_{A-X}. They were set equal to averages of lengths computed for the anti minimum. All valence angles were 109.47°. The substituent charge, the van der Waals radii of the substituents, and the r_{A-A} and r_{A-X} bond lengths were treated as variable parameters. The initial structure had the AAAA dihedral angle ω equal to 180° and the terminal groups staggered ($\phi = 0°$). Relative energies were then computed as a function of angles of rotation around the A(2)−A(3) (ω) and the A(1)−A(2) and A(3)−A(4) (ϕ) bonds, preserving a 2-fold axis of rotational symmetry.

Results and Discussion

***Ab Initio* Results for A_4X_{10}.** Since we needed to obtain results for a whole series of A_4X_{10} chains, we were limited in the quality of the calculation that we could perform. We used the HF/6-31G* approximation, which has a reasonable reputation as far as geometry optimization for ordinary molecular structures is concerned,[9b] and would be expected to give meaningful results. Intrinsic conformational barriers in simple hydrocarbon chains have been long known[31] to be describable at the Hartree−Fock level, even though the introduction of electron correlation does make some difference.[32] A comparison with the MP2/6-31G* level of calculation, which should provide a better description of nonbonded substituent−substituent interactions, is available for the potential energy curves of Si_4Me_{10}[18] and C_4F_{10}.[21] In both cases the geometries of all three conformers are nearly identical at HF and MP2 levels of calculation, the differences in the calculated potential energy curves and the relative conformer energies are small, and the unusual ortho minimum is quite pronounced. A comparison of HF and MP2 calculations for Si_4H_{10} at the 6-31G** level also revealed great similarity,[16] and the fully optimized HF/6-31G* results for the conformational minima in the A_4X_{10} series seem to be qualitatively reliable.

The HF/6-31G* results for C_4H_{10}, C_4F_{10}, C_4Cl_{10}, C_4Me_{10}, C_4Br_{10} (ECP on Br), Si_4H_{10}, Si_4Me_{10}, Si_4F_{10}, Si_4Cl_{10}, and $Si_4(SiH_3)_{10}$ are shown in Figure 1 and Table 2 (for numerical values, see Supporting Information). As anticipated,[10] the curves for the tetrasilanes are flatter than those for the butanes. Those for C_4H_{10} and Si_4H_{10} have a familiar shape and show only the expected gauche and anti minima. Most of the others look strange at first.

First, it is puzzling that the splitting of the gauche minimum into a $g_\pm$ pair and an $o_\pm$ pair, presumably[19] due to steric interactions of substituents in positions 1 and 4 (Figure 2), does not follow a simple pattern. In the carbon series, it appears upon going from an H substituent to F, and more clearly, upon going to the even larger CH_3, but then it disappears in C_4Cl_{10} and C_4Br_{10}, although the steric demands of CH_3 and Cl are normally considered to be comparable, and although Br is definitely larger than CH_3. In the silicon series, the splitting persists throughout, except for the most peculiar case of Si_4F_{10}.

Table 2. HF/6-31G* Optimized Central Dihedral Angles ω and End Group Rotation Angles ϕ in A_4X_{10} Chains (deg)

A_4X_{10}	ω_g	ϕ_g	ω_o	ϕ_o	ω_a	ϕ_a
C_4H_{10}	65.4	−3.1			180.0	0.0
Si_4H_{10}	67.2	−0.5			180.0	0.0
C_4F_{10}	56.1	−9.8	96.1	7.8	169.1	−7.7
Si_4F_{10}					133.3	−6.6
Si_4F_{10}[a]	54.9	62.3			121.3	1.8
C_4Me_{10}	52.8	−15.3	87.9	14.5	162.8	−15.7
Si_4Me_{10}	53.7	−15.3	92.0	7.7	163.5	−12.5
C_4Cl_{10}	53.0	−8.2	(90.0)[b]	6.4	156.7	−9.9
Si_4Cl_{10}	55.6	−8.0	95.8	8.6	164.6	−9.7
C_4Br_{10}	52.6	−7.6	(90.0)[b]	8.4	153.7	−9.6
$Si_4(SiH_3)_{10}$	53.4	−14.9	90.1	10.7	163.0	−15.0

[a] MP2/6-31G*. [b] There is no ortho minimum in these molecules, but the optimum geometry of the end groups is not staggered at $\omega = 90°$.

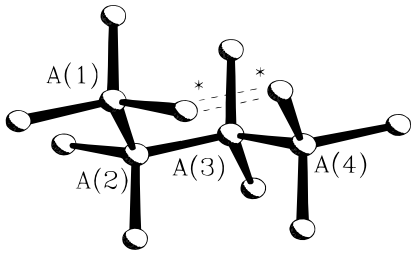

Figure 2. A schematic representation of 1,4 interactions at a geometry intermediate between gauche and ortho conformations. The substituents labeled with asterisks provide the largest contribution to the van der Waals repulsion.

Second, as ω changes from 0° to 180° (right-handed helix), the optimal value of ϕ changes in a complicated manner (Table 2): For $0° < \omega < \sim 75°$, optimized ϕ is negative ($-60° < \phi < 0°$, clockwise rotation of the end groups). The sign of optimized ϕ changes at $\omega \simeq 75°$, again at $\omega \simeq 120°$, then again at $\omega = 180°$, etc.

Third, it is noteworthy that the anti minimum is split into two ($a_\pm$) not only when repulsive interactions between substituents in position pairs 1, 3 and 2, 4[6,33] could be expected to be large, as in C_4Me_{10}, $Si_4(SiH_3)_{10}$, C_4Cl_{10}, and especially C_4Br_{10}, but also in Si_4Me_{10} and Si_4Cl_{10}, in which these steric interactions surely are small.

Since the HF results for Si_4F_{10} differed from all others, we also performed MP2 calculations. A comparison of HF/6-31G* and MP2/6-31G* results indeed revealed a qualitative difference (Figure 1), in that a shallow gauche minimum appeared only at the MP2 level. In this approximation, dispersion forces are introduced, and more compact forms such as the gauche conformer are differentially favored[16] relative to less compact forms. We believe that in all the other cases the HF/6-31G* results are qualitatively correct.

A Heuristic Model for A_4X_{10}. It is natural to assume that the puzzling behavior predicted by the ab initio calculations (Figure 1, Table 2) should be understandable in simple terms. The primary effects suited for an intuitively satisfactory rationalization are as follows: (i) an intrinsic barrier of the kind present even in ethane and disilane, (ii) repulsive or attractive van der Waals interactions between substituents, and (iii) electrostatic interactions. In the spirit of a search for simple explanations, we shall assume that these effects are additive.

An A_4X_{10} molecule that finds itself at some particular AAAA dihedral angle ω, and is strained as a result of interactions between the substituents X, will surely relieve some of the strain by modifying its other dihedral angles, valence angles, and even bond lengths. To gain simple insight into the origin of the

(31) Payne, P. W.; Allen, L. C. In *Applications of Electronic Structure Theory*, Schaefer, H. F., III, Ed.; Plenum: New York, 1977; Vol. 4, p 29.
(32) Allinger, N. L.; Fermann, J. T.; Allen, W. D.; Schaefer, H. F., III *J. Chem. Phys.* **1997**, *106*, 5143.

Table 3. Charges, Reduced van der Waals Radii, and Reduced Lateral Bond Lengths in A_4X_{10} Molecules[a]

A_4X_{10}	R_X^{vdW}	R_{AX}	r_{A-A} (Å)	r_{A-X} (Å)	q_X (au)[b]	q_X (au)[c]
C_4H_{10}	0.78[c]	0.71	1.53	1.09	+0.16	+0.20
Si_4H_{10}	0.51	0.63	2.36	1.48	−0.15	−0.18
C_4F_{10}	0.95	0.86	1.54	1.32	−0.34	−0.40
Si_4F_{10}	0.63	0.67	2.34	1.57	−0.47	−0.68
C_4Me_{10}	1.04	0.95	1.64	1.55	0.00	+0.01[d]
Si_4Me_{10}	0.72	0.81	2.36	1.90	−0.35	−0.45[d]
C_4Cl_{10}	1.07	1.09	1.63	1.78	+0.10	+0.06
Si_4Cl_{10}	0.74	0.86	2.37	2.05	−0.24	−0.39
C_4Br_{10}	1.13	1.20	1.64	1.96	+0.03	+0.15
$Si_4(SiH_3)_{10}$	0.92	0.99	2.40	2.37	+0.11	+0.08[d]

[a] Bond lengths and atomic charges are average values taken from calculations at the geometry of the anti minimum of each individual A_4X_{10} molecule. [b] Total charges on X from Mulliken population analysis. [c] Total charges on X from natural hybrid orbital population analysis. [d] Total charge on all atoms of the substituent.

number of minima observed, we have however adopted an approximation in which valence angles are always exactly tetrahedral and bond lengths are rigid, and only the AX_3 end groups are allowed to rotate away from their staggered position by an angle ϕ. This approximation is justified by the fact that the simple model is not meant to reproduce the ab initio potential energy curves quantitatively, nor are we trying to reparametrize molecular mechanics, but are merely attempting to identify the physical origin of the qualitative shape of the potential energy curves in terms of the three additive classical effects mentioned above. Not allowing other modes of motion to relax as we change ω will accentuate the root causes of changes in strain.

In keeping with the ab initio results for the conformational minima, we preserve a 2-fold axis of rotational symmetry by always rotating both end groups equally by an angle ϕ. The resulting potential energy surfaces are two-dimensional, plotted as a function of the central dihedral angle ω and the terminal dihedral angle ϕ. They were obtained for a series of parameter values reflecting (i) the nature of the intrinsic barrier as a function of A and X, (ii) the effective size of X, and (iii) the charges on A and X.

To make the model universal, we express lengths in units of the skeletal A−A bond length r_{A-A} (Table 3), and ultimately use a universal intrinsic barrier size $C = 4.5$ kcal/mol and van der Waals proportionality constant $\epsilon = 0.012$ kcal/mol. Substituent size is reflected in its reduced van der Waals radius $R_X^{vdW} = r_X^{vdW}/r_{A-A}$ and in its reduced lateral bond length $R_{AX} = r_{A-X}/r_{A-A}$. For most substituents, and all those we use, r_X^{vdW} and r_{AX}, and thus the reduced quantities R_X^{vdW} and R_{AX}, are approximately linearly related (Table 3). In the following, we refer to both values jointly as the "effective substituent size".

The question we are posing is, how does the interplay of the intrinsic barrier, the effective substituent size, and lateral bond polarity dictate the number of minima on the potential energy surface and the optimal values of ω and ϕ? We shall see below that the variation of the effects of bond polarity as a function of the dihedral angles is minimal, and we shall therefore discuss the intrinsic barrier and effective substituent size first.

(i) Intrinsic Barrier. The origin of the intrinsic 3-fold barrier to rotation in ethane has been rationalized in different ways by a series of authors,[27,34,35] and one of these had to be selected for use in the heuristic model. We decided to adopt an interpretation that goes back to Mulliken's[36] "secondary hyperconjugation" and has been convincingly advocated by Weinhold.[27] This analysis has much intuitive appeal to an organic chemist since it relates the barrier in ethane to familiar concepts such as frontier orbital theory and antiperiplanar interactions. According to this rationalization, staggered geometries are favored in ethane because they permit a more favorable stabilizing interaction of the occupied σ_{CH} orbitals of the methyl group on one end with the empty σ^*_{CH} antibond orbitals of the methyl group at the other end. The slight transfer of electron density from bonding to antibonding σ_{CH} orbitals is reflected in the somewhat longer CH bonds in ethane, r_g(CH) = 1.1108 Å,[37a] compared to methane, r_g(CH) = 1.1068 Å.[37b] This interaction also causes a slight variation in the backbone bond length and in the energy of the bonding σ_{CC} orbital as a function of ω, and this needs to be included in the analysis of barrier heights.[38]

It is quite possible that one of the other interpretations of the ethane barrier, such as the electrostatic description in terms of cumulative atomic multipole moments,[39] would work just as well, and there is a degree of arbitrariness in the choice we made.

We have computed the magnitude of the $\sigma_{CH} - \sigma^*_{CH}$ stabilizing interaction as a function of ω for all of our A_4X_{10} molecules, assuming perfectly staggered end groups AX_3 ($\phi = 0°$), and found that in all cases except Si_4F_{10} it has approximately the same functional form as in ethane, $(C/2)(1 + \cos(3\omega))$, and only the constant C varies from about 2 kcal/mol for C_4F_{10} to about 5 kcal/mol in C_4Me_{10} and about 6 kcal/mol in C_4H_{10}, C_4Cl_{10} and C_4Br_{10} (Figure 4). It thus appears that the original NBO analysis[27] of the way in which the natural bond orbital interactions vary as a function of ω applies generally. The large decrease of C from C−C bonds to Si−Si bonds is easily understood. Only the vicinal overlap of the p components of the bond and antibond orbitals contributes significantly to angular variation of the interaction, and its importance drops rapidly as one proceeds down the column of the periodic table. For tin and lead, the intrinsic barriers should be minute.

The Special Case of Si_4F_{10}. The unique very flat HF/6-31G* potential energy curve of Si_4F_{10}, with a single shallow minimum at 130° (Figure 1), resembles the familiar curve for H_2O_2.[40] The latter is usually considered to be dominated by interactions of the two oxygen lone pairs that have local π symmetry. Their nonbonded interactions are minimized at $\omega = 90°$ and maximized at 0° and 180°. The effect is believed to be further modified by the secondary effect of electrostatic repulsions between the positively charged H atoms, which are largest for $\omega = 0°$ and decrease gradually toward 180°, causing the barrier at $\omega = 0°$ to be higher than that at 180°, and shifting the minimum from 90° to 113.7°.[40] Indeed, the minimum in H_2S_2, with its long SS bond and less polar SH bonds, lies at 88.7°.[40]

(33) Anderson, J. E. In *The Chemistry of Alkanes and Cycloalkanes*; Patai, S., Rappaport, C., Eds.; Wiley: New York, 1992; p 95.

(34) Wilson, E. B., Jr. *Adv. Chem. Phys.* **1959**, *2*, 367. Radom, L.; Hehre, W. J.; Pople, J. A. *J. Am. Chem. Soc.* **1972**, *94*, 2371. Lowe, J. P. *Science* **1973**, *179*, 527. Orville-Thomas, W. J., Ed. *Internal Rotation in Molecules*, Wiley: New York, 1974. Houk, K. N.; Rondan, N. G.; Brown, F. K.; Jorgensen, W. L.; Madura, J. D.; Spellmayer, C. D. *J. Am. Chem. Soc.* **1983**, *105*, 5981.

(35) Strasburger, K.; Sokalski, W. A. *Chem. Phys. Lett.* **1994**, *221*, 129.

(36) Mulliken, R. S. *J. Chem. Phys.* **1939**, *7*, 339. Mulliken, R. S.; Rieke, C. A.; Brown, W. G. *J. Am. Chem. Soc.* **1941**, *63*, 41.

(37) Landolt, H.; Börnstein, R. *Zahlenwerte und Funktionen aus Naturwissenschaften und Technik, Gruppe II, Atom- und Molekülphysik*; Vol. 7, *Strukturdaten freier mehratomiger Molekeln*; Hellwege, K.-H., Ed.; Springer-Verlag: Berlin, Heidelberg, New York, 1976; (a) p 196, (b) p 147.

(38) Guo, D.; Goodman, L. *J. Phys. Chem.* **1996**, *100*, 12540.

(39) Sokalski, W. A.; Lai, J.; Luo, N.; Sun, S.; Shibata, M.; Ornstein, R.; Rein, R. *Int. J. Quantum Chem., Quantum Biol. Symp.* **1991**, *18*, 61.

(40) Pelz, G.; Yamada, K. M. T.; Winnewisser, G. *J. Mol. Spectrosc.* **1993**, *159*, 507 and references therein.

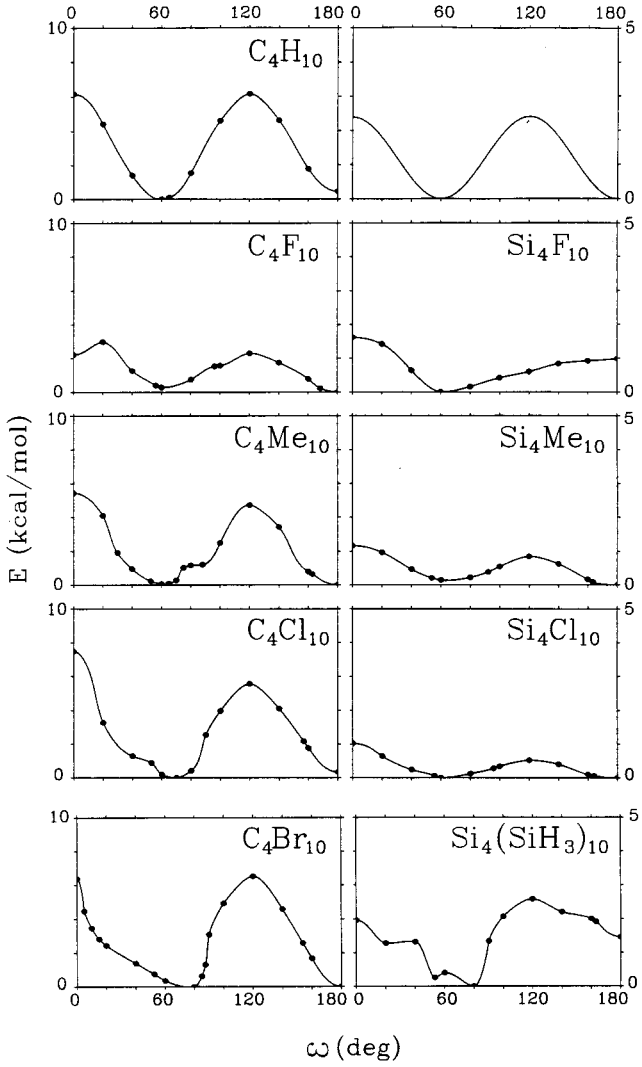

Figure 3. Ab initio computed intrinsic central rotational barriers in A_4X_{10}. The upper right corner shows the $(C/2)(1 + \cos(3\omega))$ model curve.

Not surprisingly, the NBO analysis revealed that the $\sigma_{Si-Si} - \sigma^*_{Si-F}$ interactions in Si_4F_{10} are far more stabilizing than the $\sigma_{Si-Si} - \sigma^*_{Si-Si}$ interaction. The former interaction is strongest at $\omega = 60°$ and determines the shape of the potential curve. The latter interaction is maximized at 180° but even then is so weak that it fails to induce a minimum in the curve shown in Figure 5. Finally, the addition of the effects of electrostatic repulsion, unusually large in this case, shifts the minimum in Si_4F_{10} to about 130° in the HF calculation (Figure 1).

At the MP2/6-31G* level, however, the picture for Si_4F_{10} changes, and shallow minima are present at 55° and 121°. We believe that the new gauche minimum at 55° is due to attractive van der Waals forces, which are ignored in the HF calculation. These forces normally play a minor role in A_4X_{10} compounds, because the intersubstituent distances are such that the repulsive part of the Lennard-Jones potential applies, and the HF approximation is sufficient. In Si_4F_{10} the reduced bond length R_{AX} is so small that the attractive part of the potential applies, and the HF approximation is inadequate. Clearly, the unique intrinsic barrier, the small reduced substituent bond length, and the high polarity of its bonds set Si_4F_{10} apart from all the other A_4X_{10} molecules that we have investigated.

(ii) Van der Waals Repulsions. Terminal Groups Staggered. Figure 4A shows the contribution of van der Waals

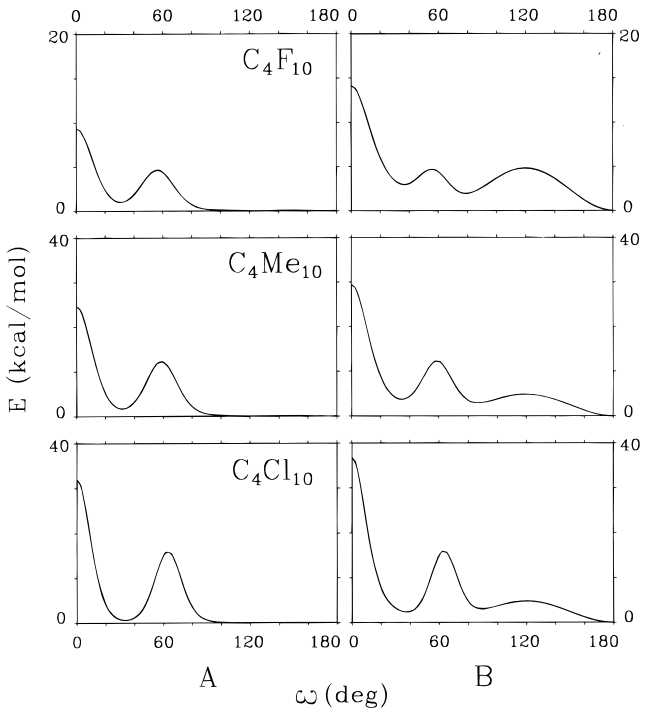

Figure 4. Model calculation: Potential energy of A_4X_{10} as a function of the dihedral angle ω, at constant $\phi = 0°$: (A) van der Waals contribution only; (B) sum of van der Waals and intrinsic contributions.

interactions between the substituents X to the total energy as a function of ω, computed using the simple model with staggered AX_3 end groups ($\phi = 0°$). In C_4H_{10}, Si_4H_{10}, and Si_4F_{10}, the effective substituent size is small enough for this contribution to be very small at all angles (these results are not shown). In the other A_4X_{10} molecules, this contribution provides an energy barrier at $\omega = 60°$, and analysis of the individual pairwise interactions shows that it is due to 1,4 interactions, as anticipated.[19]

The origin of these interactions is readily visualized. Given tetrahedral angles, at $\omega = 60°$ the four backbone atoms and two of the substituents at positions 1 and 4 form a perfect six-membered ring in the chair conformation (Figure 2). If the bonds carrying the substituents have unit length like those in the backbone, the reduced distance between the interacting 1,4 substituents is unity also, obviously much shorter than the optimal nonbonded distance $2R_X^{vdW}$. As expected, the size of the barrier at 60° increases with the increasing size of the substituent as measured by R_{AX} and R_X^{vdW}. The 1,3 interactions[19,33] are negligible, and a similar barrier is not observed to occur at $\omega = 180°$ (Figure 4).

Figure 4B exemplifies the sum of the contributions from the intrinsic and the van der Waals interactions, using an arbitrary but typical value of $C = 4.5$ kcal/mol for the former. At $\omega = 60°$, a broad well provided by the former is split by a narrower peak provided by the latter, and the gauche and ortho minima result as anticipated.[19] Together, the intrinsic and the van der Waals contributions thus account for the presence of $g_\pm$, and $o_\pm$ minima. They appear to suggest that these minima exist for all substituents X whose size is above a critical value. This disagrees with the ab initio results (Figure 1), according to which an excessive increase in substituent size removes the $o_\pm$ minimum.

Even for quite large substituents, the introduction of van der Waals interactions makes little difference in the vicinity of $\omega = 180°$. The splitting of the anti minimum to positions just

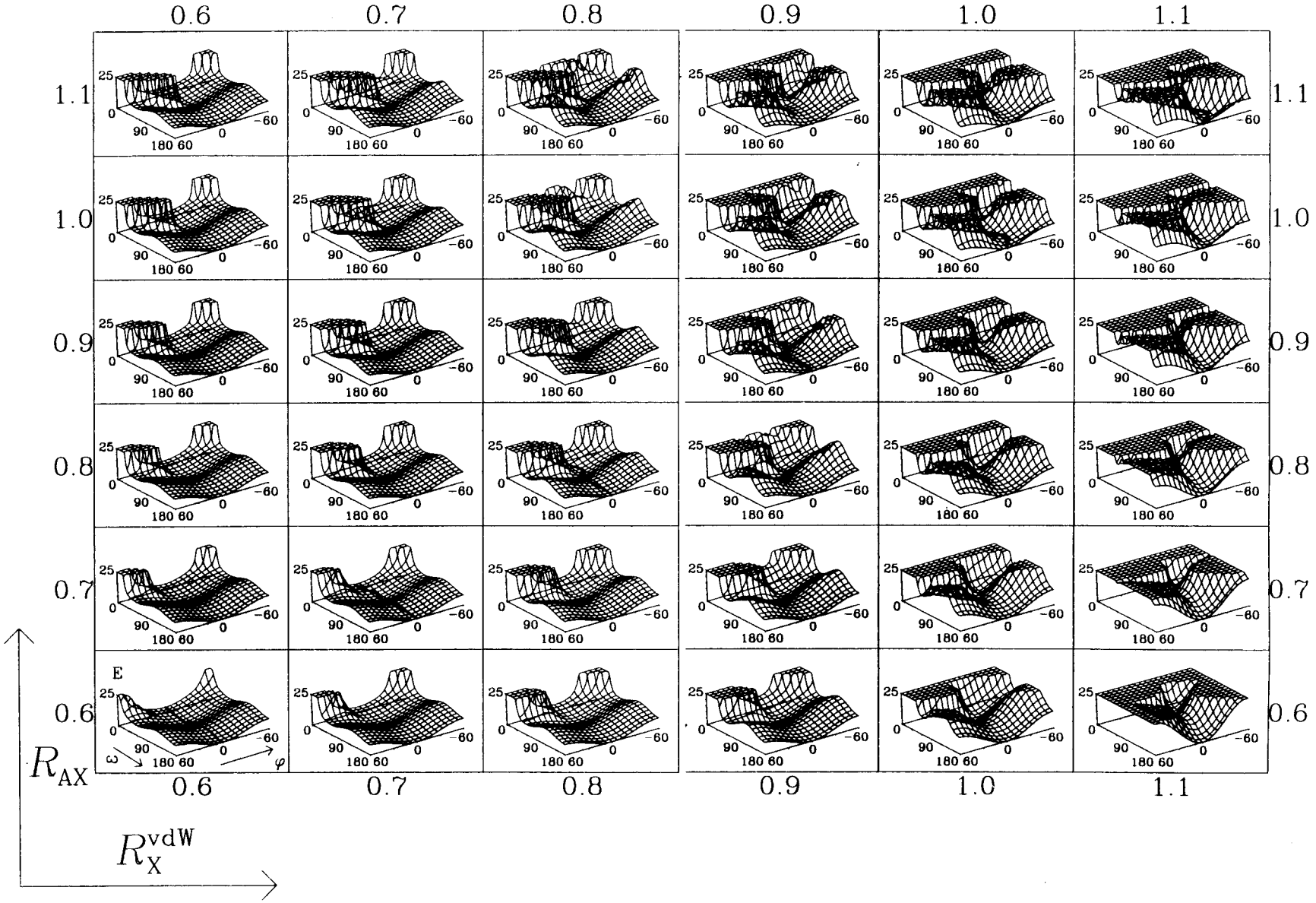

Figure 5. Model calculation: Sum of van der Waals and intrinsic ($C = 4.5$ kcal/mol) contributions to the potential energy of A_4X_{10} as a function of dihedral angle ω and end group rotation angle ϕ, reduced van der Waals radius R_X^{vdW}, and the reduced bond length R_{AX}. In drawings along the diagonal, the fat line indicates the optimal reaction path. For labels on axes, see the lower left corner.

below 180° and just above 180° thus cannot be explained by this simplest approach, in which the end groups are forced to remain staggered.

Terminal Group Rotation. To understand the factors that control the splitting of the gauche minimum into two, we examined the role of the rotation of the terminal AX_3 groups (dihedral angle ϕ), whose importance has been well recognized.[6,19,33] According to the ab initio results (Table 2), these groups are not perfectly staggered in most of the A_4X_{10} conformational minima. They are twisted counterclockwise in the region of the ortho minimum (o_+), between the transition state that leads to the gauche form and the one that leads to the anti form, and clockwise in the regions of the gauche (g_+) and twisted anti (a_+) minima. The twist directions are inverted for the g_-, o_- and a_- minima ($0° \geq \omega \geq -180°$). As ω increases in a A_4X_{10} molecule with 6 minima, the sense of end group rotation thus reverses each time the molecule passes through a transition state that separates conformers. In the compounds with 4 minima, C_4Cl_{10} and C_4Br_{10}, the sense of twisting changes as if the transition states defining the ortho minimum were still present.

Figure 5 shows a series of plots of energy calculated from the simple model as a function of both the central AAAA dihedral angle ω from 0° to 180° (results for $0° \geq \omega \geq -180°$ follow from symmetry), and the angle ϕ, related to the terminal AAAX dihedral angle, from $\phi = 0°$ (staggered) to $\phi = 60°$ (counterclockwise rotation, eclipsed) or $\phi = -60°$ (clockwise rotation, eclipsed). The individual plots in Figure 5 differ in effective substituent size as defined by R_X^{vdW} and R_{AX} (Table 3). The energy contains additive contributions from van der Waals interactions, from the intrinsic barrier at the central bond, $(C/2)(1 + \cos(3\omega))$, and from the intrinsic barriers at the two terminal bonds, which add up to $C(1 - \cos(3\phi))$.

Instead of the simple one-dimensional representation of the conformational isomerization path implied in Figure 4, in Figure 5 we consider a path represented by a curve of minimal energy that winds its way over the ω,ϕ plane and connects the minimum at the $\omega = 0°$ edge with the minimum at the $\omega = 180°$ edge for each choice of R_X^{vdW} and R_{AX}.

Since we assume rigid rotation, while the real molecule relieves some strain by adjusting bond lengths and valence angles, strong interactions already occur for smaller effective substituent sizes in the model than they do in reality. This does not reduce the utility of the plots for a discussion of the origin of trends in the conformational effects of substituent size, and merely means that the effective substituent size, i.e., the values of R_{AX} and R_X^{vdW}, need to be taken smaller than would be expected from standard tables; e.g., instead of taking the proper values of $R_{CCl} = 1.08$ and $R_{Cl}^{vdW} = 1.10$, we need to take an effective value of about $R_{CCl} \cong R_{Cl}^{vdW} \cong 1.0$ to approximate the ab initio result.

The Gauche and Ortho Minima. To understand the role of the rotation of the end groups in the ortho and gauche minima, we refer to Figure 2, in which the A_4X_{10} molecule is shown with staggered end groups, at $(\omega,\phi) = (60°,0°)$. The substituents on A(4) and A(1) responsible for the repulsive 1,4 interaction (see Figure 4) are marked with an asterisk. Their separation can be increased and the 1,4 interaction strain can be relieved at the expense of a loss of perfect staggering at the terminal bonds. Achieving this by clockwise rotation of AX_3 groups around the terminal A−A bonds amounts to optimizing the geometry of the gauche minimum (right-handed helix, $0° \leq \omega \leq 70°$, Figure 6A). Doing it by counterclockwise rotation of the AX_3 groups results in the optimization of the geometry of the ortho minimum ($\omega \cong 80-90°$, Figure 6B). The clockwise rotation of the AX_3 groups from the perfectly staggered position in the gauche form of the right-handed helix ($\phi < 0$) and their counterclockwise rotation in its ortho form ($\phi > 0$) are hallmarks of these minima. The simultaneous rotation of both end groups by ϕ preserves C_2 symmetry.

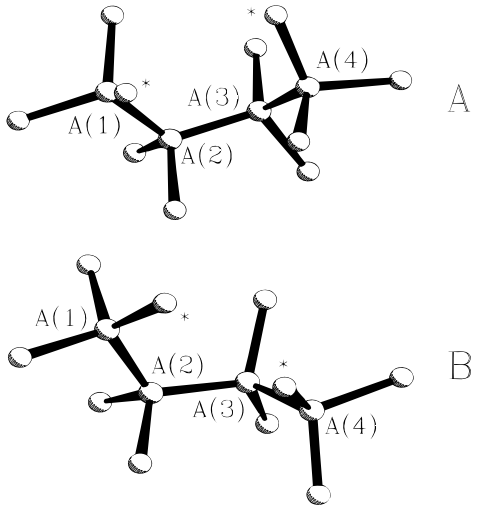

Figure 6. Gauche (A) and ortho (B) geometry of A_4X_{10}.

Next, we return to Figure 5 and start with the smallest substituents, located in the lower left corner ($R_{AX} + R_X^{vdW} \leq 1.4$, Table 3). The minimum energy isomerization path is not affected by van der Waals repulsions between substituents at all and goes only through the gauche and anti minima, both at $\phi = 0°$. Rotation of the terminal groups away from the staggered arrangement to either positive or negative values of ϕ increases the energy because of intrinsic barriers at both terminal bonds. If $R_{AX} + R_X^{vdW} > 1.4$, increasing 1,4 interactions cause a twisting of the end groups from the staggered arrangement, as can be seen for $R_{AX} = R_X^{vdW} = 0.8$. At this point, the surface still contains only a gauche minimum at $\omega \simeq 60°$, with $\phi < 0°$, an anti minimum at $\omega = 180°$, and no ortho minimum.

As noted above, repulsive van der Waals interactions are also absent in Si_4F_{10}, but Figure 5 is not applicable, because this special case has a different intrinsic barrier function.

Going to the next group of compounds, C_4F_{10}, Si_4Me_{10}, C_4Me_{10}, Si_4Cl_{10}, and $Si_4(SiH_3)_{10}$, the effective substituent size is increased enough that the sum $R_{AX} + R_X^{vdW}$ exceeds 1.5 but is still smaller than 1.9. As the effective substituent size increases, a high-energy ridge due to 1,4 interactions gradually develops in the potential energy surface and protrudes from the point $(\omega,\phi) = (0°,60°)$ toward the center point of the plot (90°,0°). In doing so, it displaces the minimum energy isomerization path further to negative values of ϕ in the region of the gauche minimum. At the same time, increasing 1,3 interactions introduce additional hills into the surface at $(\omega,\phi) = (120°, 60°)$ and $(120°,-60°)$, displacing the minimum energy path toward positive values of ϕ near $\omega = 90°$ and toward negative ones at $\omega \geq 120°$. As the values $R_X^{vdW} = R_{AX} = 0.9$ are reached, the above-mentioned ridge merges with the hill that grew at $(\omega,\phi) = (120°,-60°)$, creating a barrier that separates the original gauche minimum into an ortho and a gauche minimum. This is the barrier that so clearly appeared in Figure 4 at $\omega = 60°$. These compounds have six conformational minima.

Additional increase in effective substituent size ($R_X^{vdW} + R_{AX} \geq 2.0$) leads to further increase of the hills and ridges in

the potential energy surface. The ridge due to 1,4 interactions, which started from the point $(\omega,\phi) = (0°,60°)$, and the hill due to 1,3 interactions, which grew at $(\omega,\phi) = (120°,60°)$, start to obliterate the ortho minimum and make it disappear when R_{AX} and R_X^{vdW} approach unity. The valley that contained this minimum then spills its content into the wide well that contains the anti minimum. This is the reason for the presence of only four minima in C_4Cl_{10} and C_4Br_{10}. A closer examination of Figure 1 indeed reveals a shoulder at $\omega = 100°$ for C_4Cl_{10}. The unusual flat region between $\omega = 90°$ and 120° presumably is the remnant of the former ortho minimum. In C_4Br_{10} the reduced substituent size has increased sufficiently that even the last hint of an ortho minimum has vanished. For such large substituents the barrier that separates the gauche valley from the unified ortho + anti valley is massive, and passage over its lowest point difficult. The minimum energy path is displaced toward negative values of ϕ, except in the region of $75° \leq \omega \leq 120°$, where memory of the ortho valley survives and ϕ is positive.

The methyl group can decrease its effective van der Waals radius by meshing with other methyl groups in a gearing motion[6,33] and effectively has a smaller R_{AX} value than chlorine, which does not have this option (Table 3). Apparently, the effective size of the methyl groups lies just below the critical limit, so C_4Me_{10} still has all six minima. C_4Cl_{10} is located just above the critical value, at which the ortho minimum is lost.

We conclude that the existence of the ortho minimum is precarious and is dictated by two critical effective substituent sizes. As X increases upon going from the lower left to the upper right in Figure 5, the gauche minimum first splits into a gauche and an ortho minimum, and then the ortho minimum disappears by merging with the anti minimum.

The Anti Minimum. Due to significant 1,3 interactions, for very large substituents the energy surface is warped between $\omega = 170$ to 180° and $\phi = 0$ to −60° (Figure 5) and develops a well at $(\omega,\phi) \simeq (170°,-10°)$. Thus, at $R_{AX} \simeq R_X^{vdW} \simeq 1.1$, the anti minimum splits and moves from $(\omega,\phi) = (180°,0°)$ to $(\omega,\phi) \simeq (170°,-10°)$. In this region of geometries steric interactions are relatively weak. It is reasonable to assume that there are no great distortions from the ideal geometry with tetrahedral angles, and the R_X^{vdW} and R_{AX} values are realistic. Thus, in the cases of C_4Me_{10}, C_4Cl_{10}, and C_4Br_{10}, and marginally C_4F_{10}, we can explain the origin of the split anti minimum in terms of 1,3 van der Waals repulsions. However, the ab initio calculations predict a split anti minimum even in many less hindered compounds, such as Si_4Cl_{10} and Si_4Me_{10}, and the simple model does not.

A related puzzle is the twisting[6,33] of the end groups away from perfect staggering in the anti minimum valley. This is clearly obtained in the ab initio results not only for the largest substituents, but also for those with R_X^{vdW} and R_{AX} values for which Figure 5 does not suggest any deviations from $\phi = 0°$. This could be understood as one way to relieve the steric 1,3 repulsions, and perhaps Allinger et al.[30] were right in suggesting that van der Waals radii are substantially larger than is normally assumed. But even in Si_4F_{10}, where steric 1,3 repulsions can hardly be invoked, the end groups are twisted away from a perfectly staggered geometry when ω is fixed at 160° and the other degrees of freedom are relaxed. It seems to us that direct 1,3 steric interactions can be only partially responsible for the twisting of end groups in molecules with moderate or large R_{AX} and R_X^{vdW} values, and that there must be an additional reason for this quite prevalent phenomenon. We suspect that it is related to nonadditivity of the orbital interactions that are responsible for intrinsic barriers (cf. Supporting Information).

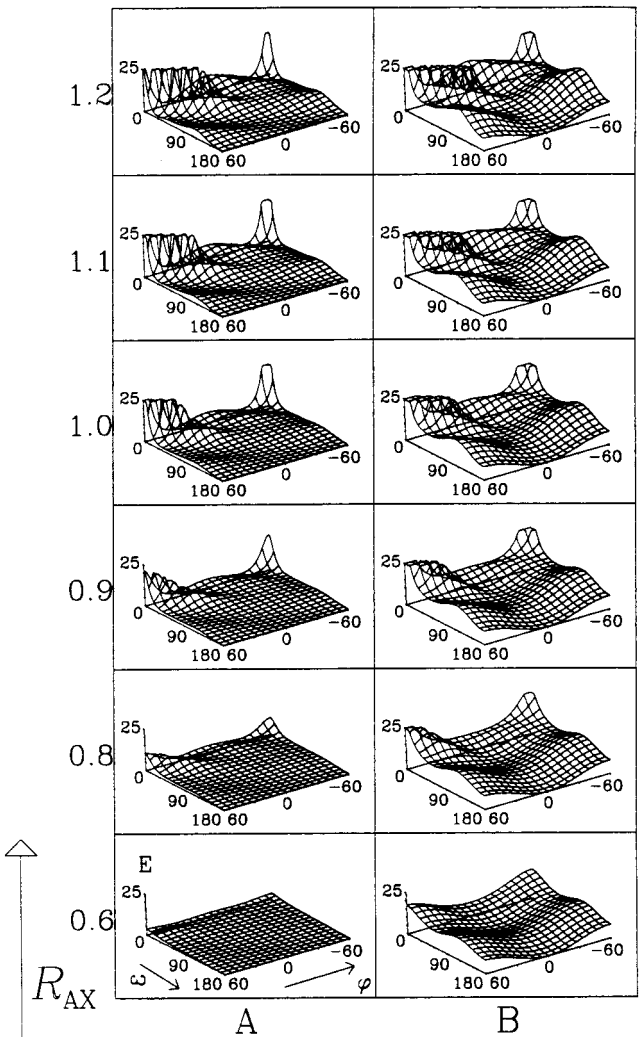

Figure 7. Model calculation: Electrostatic contribution to the potential energy of A_4X_{10} chains as a function of dihedral angle ω, end group rotation angle ϕ, and the reduced bond length R_{AX}. Left: Electrostatic interaction alone. Right: Electrostatic interaction plus intrinsic barrier ($C = 4.5$ kcal/mol). For labels on axes, see the lower left corner and text.

(iii) Electrostatic Interactions. Figure 7 shows the electrostatic repulsion energy as a function of the dihedral angles ω and ϕ for a series of reduced bond lengths R_{AX}. The AX bonds carry opposite charges $q_X = \pm 0.2$ *e* at each end. For other values of q_X (Table 3), the interaction energy scales as q.[2] For an AA bond length of 1.0 Å, the vertical scale is in kilocalories per mole; for other AA bond lengths *r*, it scales as $1/r$.

One could take issue with some of the charges calculated, either by the Mulliken or Weinhold methods. Thus, in C_4Cl_{10}, the chlorine atoms are calculated to carry positive charges, and the carbon atoms are negatively charged. This might be a problem of an inadequate basis set,[41] and these calculations were therefore repeated at the 6-311G* level. However, although the magnitudes of the charges were reduced somewhat, no significant changes in the potential energy curve or the intrinsic barrier resulted.

For realistic bond length ratios and bond dipoles, the electrostatic interaction energy does not depend on dihedral angles in a way conducive to producing minima or barriers in

(41) Jug, K.; Köster, A. M. *Int. J. Quantum Chem.* **1993**, *48*, 295.

the potential energy surface. Even in the most polar case, Si_4F_{10} [q_F(Mulliken) $\simeq -0.47$ *e*, q_F(NBO) $= -0.68$ *e*, $R_{AX} = 0.67$], the electrostatic repulsion energy is a roughly linear function of ω and is nearly constant with respect to the end group rotation ϕ (Figure 7). All our investigations of the electrostatic contributions to the barriers suggest that they are not essential for the understanding of conformational properties of A_4X_{10} chains. This is not surprising, considering the weak $1/r$ dependence of the electrostatic potential on distance.

Beyond the Simple Model. Additive intrinsic barriers, van der Waals interactions, and electrostatic interactions, combined with rigid rotations, account quite satisfactorily for the splitting of the gauche minimum as a function of substituent size, and the model has thus accomplished its main purpose. It has however accounted less well for the more familiar weak splitting of the anti minimum and for the twisting of the end groups. Although it leaves little doubt that 1,3 van der Waals interactions are responsible for these phenomena when X is large, both occur for smaller substituents than expected. Perhaps the commonly used van der Waals radii are too small,[30] but it appears likely that the discrepancy has additional causes, such as more subtle properties of intrinsic barriers and geometrical changes during the rotations. After all, although in an infinite chain the intrinsic barriers would be the same for all AA bonds, in an A_4X_{10} molecule the central and the terminal bonds are clearly different and do not have identical intrinsic barrier heights. Even in an infinite chain, the intrinsic barriers do not have 3-fold symmetry since the AX and AA bonds are inequivalent. The additivity of the intrinsic barriers is questionable, since in the Weinhold picture two donor orbitals competing for a single acceptor orbital will not be twice as successful as a single donor orbital interacting with a single acceptor orbital.

In Supporting Information we propose that van der Waals repulsions have a double effect on the rotational isomerization pathway of an A_4X_{10} molecule. A bigger substituent causes higher repulsions directly, and it also induces valence angle changes that affect hybridization and modify the intrinsic barrier. Thus, van der Waals repulsions could force a splitting of the anti minimum even when the substituent size is relatively moderate.

Conclusions

With the sole exception of Si_4F_{10}, the main conformational properties of the A_4X_{10} molecules studied can be understood in terms of the intrinsic barrier as defined by Weinhold's procedure, and of standard van der Waals radii. The often ignored splitting of the gauche minimum into gauche and ortho is general. It is confirmed to be due to 1,4 van der Waals interactions as previously proposed, but is now predicted to appear only for a certain range of substituent sizes (R_X^{vdW} and R_{AX} between 0.8 and 1.0 in units of backbone bond length). The twisting of the anti minimum away from 180° (i.e., its splitting) is due to 1,3 van der Waals interactions as previously believed, but appears already at smaller substituent sizes than expected. There could be several reasons for this and one is examined briefly in the Supporting Information. It suggests that even relatively small changes in valence angles induced by the 1,3 interactions amplify the steric effect of the substituents by affecting hybridization on the backbone atoms and thus flattening the intrinsic barriers that favor perfect staggering.

Acknowledgment. This paper is dedicated to the memory of Prof. Michael J. S. Dewar. Work performed at Colorado was supported by USARO grant DAAH04-94-G-0018, funded jointly with NSF/DMR, and by NSF grants CHE-9412767 and CHE-9318469. F.N. is grateful to the Alexander von Humboldt Foundation for a Feodor Lynen Fellowship. Work performed at Kanagawa was supported by NTT, Inc. We thank Mr. Dean Antic for performing some of the calculations for C_4F_{10}.

Supporting Information Available: Table of the numerical results displayed in Figure 1; results for and discussion of the origin of the splitting of the anti minimum and of the twist of the terminal groups, with Figures 8−12 (13 pages). See any current masthead page for ordering and Internet access instructions.

JA971406N